Topography quantifications allow for identifying the contribution of parental strains to physical properties of co-cultured biofilms

Elif N. Hayta [a,b], Carolin A. Rickert [a,b], Oliver Lieleg [a,b,*]

[a] Munich School of Bioengineering and Department of Mechanical Engineering, Technical University of Munich, 85748, Garching, Germany
[b] Center for Protein Assemblies (CPA), Technical University of Munich, Ernst-Otto-Fischer Straße 8, 85748, Garching, Germany

ARTICLE INFO

ABSTRACT

Most biofilm research has so far focused on investigating biofilms generated by single bacterial strains. However, such single-species biofilms are rare in nature where bacteria typically coexist with other microorganisms. Although, from a biological view, the possible interactions occurring between different bacteria are well studied, little is known about what determines the material properties of a multi-species biofilm. Here, we ask how the co-cultivation of two *B. subtilis* strains affects certain important biofilm properties such as surface topography and wetting behavior. We find that, even though each daughter colony typically resembles one of the parent colonies in terms of morphology and wetting, it nevertheless exhibits a significantly different surface topography. Yet, this difference is only detectable via a quantitative metrological analysis of the biofilm surface. Furthermore, we show that this difference is due to the presence of bacteria belonging to the 'other' parent strain, which does not dominate the biofilm features. The findings presented here may pinpoint new strategies for how biofilms with hybrid properties could be generated from two different bacterial strains. In such engineered biofilms, it might be possible to combine desired properties from two strains by co-cultivation.

Introduction

With the first cry of a baby, an endless debate starts: Does he/she resemble mom or dad? Not only seem all relatives to have a different opinion on this topic, the question itself appears to be ill-conceived. Clearly, every child has inherited certain traits from both of his parents, and subjective 'morphological' classifications by an 'expert panel' are not sufficient to detect the parents' contributions. Similarly, simple morphological descriptions of other biological entities can be misleading. For instance, *Myrmarachne formicaria*, an animal known as ant-like jumping spider (which was chosen as the "spider of the year 2019" by the European Society of Arachnology) is famous for its incredible capability of mimicking ants [1]. Often enough, those spiders cannot be distinguished from ants by an unexperienced observer, and sometimes even quantitative approaches are required to assign them correctly [2].

A famous case from material science, where a quantitative characterization is required to achieve a correct categorization is the wetting properties of superhydrophobic surfaces. For instance, both rose petals and lotus leaves exhibit superhydrophobic surfaces with extremely high contact angles; yet, they are still different from each other in terms of

droplet adhesion: water droplets strongly adhere to rose petals but easily roll off from lotus leaves [3]. Whereas this is a qualitative criterion, a more detailed quantification procedure (i.e., a contact angle hysteresis measurement) correctly classify a surface as rose-like or lotus-like [3,4].

The wetting behavior of a material is dictated by a combination of surface chemistry and topography [5,6]. For a superhydrophobic surface, low surface energy and hierarchical roughness features in the micro- and nanoscale are required [6,7]. A detailed relation between the wetting behavior and the surface topography has also been demonstrated for biofilms – a special form of surface-attached bacteria which are embedded into a matrix of secreted macromolecules [8]. Also, the susceptibility of biofilms towards antibiotic solutions, their resilience to other chemical stresses and the erosion resistance of biofilms were shown to be related to the surface topography of those soft materials [9,10]. In fact, in recent years, quantitative topographical analyses of biofilms have become a well-established and useful tool in biofilm research [8,10–15].

The vast majority of biofilm properties studied to date is critically related to the extracellular polymeric substances (EPS) secreted by the bacteria [11,16,17]. Interestingly, even when bacterial strains belong to the same species, the biofilms they produce may differ in terms of EPS

composition. For instance, the matrix of *B. subtilis* NCIB 3610 biofilms contains exopolysaccharides expressed by the *eps*A-O operon [18], an amyloid-fiber-forming protein *Tas*A [19,20], and a surface layer hydrophobin, *Bsl*A [21,22] – the latter of which is required for the biofilms to develop hydrophobic properties. In contrast, *B. subtilis natto* and B-1 biofilms are mostly composed of γ-polyglutamate [23,24]. Previous studies demonstrated that those different matrix components affect biofilm properties in different ways, and biofilms generated by different variants of *B. subtilis* bacteria show very different physical properties – which is due to their unique matrix compositions and surface topographies [8,11,22].

Whereas biofilms cultivated in the lab for research purposes are typically generated from one particular bacterial strain only, naturally occurring biofilms such as dental plaques or biofilms used in biotechnology, e.g. for wastewater treatment, typically contain a multitude of several bacterial strains [25–30]. Such multi-species biofilms, i.e., microbial communities, where more than one strain is present at the same time, will exhibit features and properties which are brought about by the detailed mixture of strains involved [28]. Hence, throughout this manuscript, we use the phrase 'parent' to describe single strains contributing to the properties of co-cultured colonies; following the same logic, those co-culture colonies are referred to as 'daughters' to indicate that they possess hybrid properties brought about by the 'parents'. We emphasize that those terms are not supposed to indicate an inter-generation dependency of the strains used here.

Interspecies interactions within co-cultured biofilms have already been investigated in detail, and different aspects such as the spatial organization of colonies, quorum sensing, evolution or biofilm control by competing bacteria have been analyzed [31–40]. Paul et al. (2019) [41] investigated the inter-colony interactions of two 'sibling' *B. subtilis* colonies by qualitatively analyzing their morphology; they concluded that these sibling colonies either merge or form demarcation lines – depending on how the detailed nutrient supply and starting distance of the sibling colonies were chosen. However, a follow-up study conducted at the cellular level by Matoz-Fernandez et al. (2020) [42] showed that the two sibling strains actually did not merge but remained spatially separated. Together, these studies indicated that attempting colony classifications based on macro-scale information alone might be insufficient.

Here, we show that the binary mixtures of *B. subtilis* NCIB 3610, *natto* and B-1 strains exhibit microscopic surface topographies and wetting behavior that are similar to those of their morphologically dominating parent colonies – but still distinct from them. However, this distinctiveness of the daughter colonies is not obvious enough to be detected by a macromorphological evaluation via computational image comparison approaches or by an untrained examination panel. In contrast, it requires a metrological quantification of the colony surfaces on the microscopic level. Interestingly, in all but one mixtures, the parent strain dominating the daughter colony properties is also found in larger numbers than the other, dominated parent strain. Our findings suggest that topographical analyses as we conduct them here can be a helpful tool to investigate the properties of co-cultured biofilm colonies, where the behavior of the colonies is determined by the detailed mixture of bacterial strains generating the biofilm colony.

Materials and methods

If not stated otherwise, chemicals were purchased from Sigma Aldrich (St Louis, USA).

Biofilm colony formation

Planktonic cultures were generated as described in the SI. To obtain biofilm colonies, 16 h old planktonic cultures were first diluted to an OD_{600} of 0.6 using fresh LB medium. For creating binary mixtures of NCIB 3610/*natto*, NCIB 3610/B-1 and *natto*/B-1, respectively, the diluted planktonic cultures were mixed at a volumetric ratio of 1:2, 1:4 and 1:2, respectively; those mixture ratios were chosen to obtain mixtures containing equal numbers of viable cells from each strain (see main text). By doing so, we aim to create fair conditions where both bacterial strains have equal chances to contribute to the properties of the co-cultured biofilm colony. Then, five separate 5 μL drops of these mixtures (or standard cultures of NCIB 3610, natto and B-1 diluted to the same OD_{600}) were placed onto 1.5% (w/v) agar plates enriched with either 2.5% (w/v) of LB or MSgg (Minimal Salts Glycerol Glutamate) media. The MSgg medium contained 5 mM potassium phosphate, 100 mM 3-(N-Morpholino)propanesulfonic acid (MOPS) (Carl-Roth, Karlsruhe, Germany), 2 mM $MgCl_2$, 700 μM $CaCl_2$, 50 μM $MnCl_2$, 50 μM $FeCl_3$, 1 μM $ZnCl_2$, 2 μM thiamine, 0.5% (v/v) glycerol, 0.5% (w/v) glutamate, 50 μg/mL L-tryptophan, 50 μg/mL L-phenylalanine, and 50 μg/mL threonine. The inoculated agar plates were incubated at 37 °C and ~25% humidity for 1 day, and we conducted all analyses on these 1 day old colonies to obtain colonies that are large enough for accurate contact angle and surface topography measurements. These co-cultured colonies were not studied at later time points of cultivation to avoid bacterial competition effects within the colony – which would further increase the complexity of the experimental outcome.

Biofilm colony classification based on macromorphological appearance

To assign a morphologically dominating 'parent' to each of the co-cultured biofilm colonies, a panel comprising nine people was asked to select the most similar 'parent' colony among three single strain colonies of *B. subtilis* NCIB 3610, *natto* and B-1 strains. The strain that had received the most votes was then selected as the 'dominating parent'; in the case of tied votings, the respective co-cultured colonies were classified as 'inconclusive'.

Similar to the panel survey, three different computational approaches were employed to classify the images of the co-cultured biofilms according to their similarity to pure, one-strain 'parent' colonies. In detail, all images were subjected to a pairwise comparison with one of three reference colony images (one per bacterial 'parent' strain), and the best-matching parent colony was considered as the algorithm's decision. For this comparison, the following methods were applied: First, the structural similarity [43] metric was used, which performs a generic image comparison that estimates the perceived difference of two images; second, template matching based on correlation coefficients was conducted; third, oriented FAST and rotated BRIEF (ORB [44]) – a robust local feature detector based on the FAST [45] (Features from Accelerated Segments Test) key point detector and a modified version of the visual descriptor BRIEF [46] (Binary Robust Independent Elementary Features) – was used (for more detailed information please see the Supplementary Information). All algorithms were programmed and executed with Python (version 3.8.3, Python Software Foundation, Wilmington Delaware, USA) including the NumPy [47] (version 1.19.2) extension for numerical calculations. For image handling and preprocessing, OpenCV [48] (Open Source Computer Vision Library, version 4.4.0), Pillow [49] (version 8.0.1) and Scikit-image [50] (version 0.17.2) Toolboxes were used.

Biofilm wetting properties

To determine the wetting behavior of the center of biofilm colonies, water droplets (2.5 μL or 5 μL in volume; the volume of the droplets had to be adjusted in dependency of the hydrophobicity and size of the biofilm colonies) were placed onto the surface of NCIB 3610, *natto* and B-1 biofilms, respectively. Then, transversal images of those water droplets were acquired using a high-resolution camera (Point Grey Research, Richmond, Canada). Finally, contact angle values were determined by processing the images with the "drop snake" plug-in of the OpenSource software ImageJ.

To distinguish between rose-like and lotus-like superhydrophobicity, the biofilm colonies were tilted after the contact angle measurement. The

colonies were designated as rose-like if the droplet remained attached to the biofilm surface during tilting; conversely, the colonies were rated lotus-like when the droplet rolled-off upon sample tilting.

Topographical biofilm characterization on the micro-scale

As in previous work, the microscopic surface topography of the biofilm colonies was characterized using optical profilometry [8,10]. In detail, topographical images were acquired from the central areas of the biofilm colonies using a 3D laser scanning confocal microscope (VK-X1000 series, Keyence Corporation, Osaka, Japan) at $20\times$ magnification resulting in image sizes of 529 μm × 705 μm comprising 2048 × 1536 pixels. The step size in z was 0.5 μm, and the corresponding resolution in this dimension (based on fitting algorithms employed by the software) was 0.5 nm. The obtained topographical data was then evaluated with the software MultiFileAnalyzer (Version 2.1.3.89, Keyence Corporation, Osaka, Japan).

To quantify the surface topography of the biofilm colonies, different topographical parameters were calculated, which are all defined in ISO norm 25178. In this study, we mainly focus on the developed interfacial surface ratio,

$$Sdr = \frac{1}{A} \left[\iint_A \left(\sqrt{\left[1 + \left(\frac{\partial z(x,y)}{\partial x}\right)^2 + \left(\frac{\partial z(x,y)}{\partial y}\right)^2\right]} - 1 \right) dxdy \right],$$

which describes the ratio of the measured surface area (as established by the surface texture) with respect to the (perfectly flat) definition area. This *Sdr* parameter was previously shown to be suitable to differentiate between different complex topographies of biofilms, which are related to differences in their wetting properties [8]. However, for some specific cases, a more in-depth analysis employing additional metrological parameters were required (see supplement for details).

Optical microscopy

The presence of *B. subtilis* NCIB 3610, *natto* and B-1 bacteria within co-cultured colonies was investigated by a combination of fluorescence and phase-contrast microscopy. In those experiments, we used a modified NCIB 3610 strain that expresses the green fluorescent protein (GFP). As similar GFP-expressing *natto* and B-1 strains were not available to us, only binary mixtures containing NCIB 3610 could be studied. Prior to preparing fluorescently labeled colonies, we quantified the number of viable NCIB 3610-GFP bacteria at an OD_{600} of 0.6 and compared this value to numbers obtained for standard NCIB 3610 bacteria grown at the same conditions. There was no significant difference ($p = 0.155$) between wild-type and GFP expressing ((3.9 ± 0.3) x 10^8 CFU/mL) strains. Also, both variants of this bacterial strain exhibit similar growth kinetics in LB and MSgg media (Fig. S3). Co-cultured biofilm colonies of NCIB 3610-GFP/B-1 and NCIB 3610-GFP/*natto* were obtained as described above. Then, a piece of biofilm sample was taken from the center of the colonies, transferred into 100 μL of distilled water and vortexed to ensure a homogeneous bacterial solution. 5 μL of this homogenized bacterial suspension was then placed onto μ-slide wells (Ibidi, Planegg, Germany) and covered with an agarose patch of 600 μm thickness. The mixture of fluorescent (NCIB 3610) and non-fluorescent (either *natto* or B-1) bacterial cells was then visualized on an inverse light microscope (Leica Biosystems, Hesse, Germany) at $63\times$ magnification using a digital camera (Orca Flash 4.0 C11440–22C, Hamamatsu, Japan) at 2×2 binning in two ways: first, using a FITC filter; second, in phase-contrast mode. The acquired images were then processed with Image J as follows: First, the backgrounds of both images were removed. Their brightness intensities were equalized, and the images were merged and converted into RGB values. Then, the composed images were split again, and any unevenness resulting from the background of the phase-contrast images was smoothened by applying a bandpass filter. These grey-scaled phase-

contrast images were colored by Lookup Tables (LUT), and then the LUT was inverted. The brightness of the images was adjusted to select cells. The total number of cells was determined using a color threshold and the particle analysis plug-in of ImageJ. Then, GFP-expressing (=NCIB 3610) cells were identified from the merged images and counted. The number of non-fluorescent bacteria (= *natto* or B-1) was obtained by subtracting the number of fluorescent (NCIB 3610) cells from the total number of bacteria.

Sample sizes and statistics

For morphological observations, surface topography analysis and contact angle measurements, we obtained data from 15 individual samples generated from three independent growth batches. For fluorescence imaging, all data was obtained from 10 individual samples created from two distinct growth batches. For all sample subgroups (e.g., *natto*-like samples, 3610-like samples, B-1-like samples), data from at least 3 technical replicates and a minimum of 5 individual samples was collected and analyzed.

A statistical analysis of the data was performed using the software SigmaPlot 12.5 (Systat Inc, San Jose, CA, USA). Statistically significant differences between samples were assessed by performing two-sample t-tests assuming a two-tailed alternative hypothesis with a confidence level of 95%. The assumptions of normal distribution and equal variances were also tested with this software ($p = 0.05$).

To assign a 'least different' parent strain to each of the individual co-cultured colonies generated from NCIB 3610/*natto* mixtures, we applied pairwise t-tests using the open source software R. Then, we compared the *Sdr* or contact angle data obtained from 3 technical replicates for each individual co-cultured colony to those of three single strain 'parent' colonies. Holm's method was employed to control the family-wise error [51]. Different from standard t-tests, here, we then applied a reverse approach, i.e., we identified the highest *p*-value within each set of compared samples of 'parent' and 'daughter' colonies and selected the corresponding 'parent' strain, accordingly. The corresponding results are shown in the SI.

Results

When three different strains of *B. subtilis* are grown separately on LB agar (at 37 °C with ~25% humidity for 1 d), the obtained colonies differ in terms of morphology and wetting behavior (Fig. 1). Whereas *B. subtilis* NCIB 3610 and *natto* strains form hydrophilic colonies with smooth surfaces, *B. subtilis* B-1 colonies exhibit extremely liquid repellent (= superhydrophobic lotus-like) surfaces with micro- and macroscopic roughness features. We here ask if mixtures of those strains would generate colonies with new surface features, or if the properties of one of the 'mother' colonies were to dominate the outcome.

To obtain a controlled mixture of *B. subtilis* NCIB 3610, *natto* and B-1 strains, one possibility would be to adjust the densities of the overnight cultures to the same value before mixing. However, this approach does not necessarily guarantee similar amounts of living cells in these suspensions: when bacterial liquid cultures reach the stationary phase, they contain not only living and dead cells but also microbial debris and secreted metabolites – and all of these components may contribute to the optical density of the culture [52]. Thus, to obtain starting conditions that allow us to mix similar numbers of bacteria generated from the three different strains, we first determine the CFUs of bacterial overnight cultures at different optical densities (Fig. S2). Indeed, 16 h old cultures of *B. subtilis* NCIB 3610, *natto* and B-1 diluted to an OD_{600} of 0.6 contain (4.4 ± 0.5) x 10^8, (2.0 ± 0.4) x 10^8 and (1.3 ± 0.4) x 10^8 CFU/mL, respectively. Even though those differences are not huge, this result demonstrates that mixing bacterial cultures at the same optical density would create somewhat unfair starting conditions within the colony as always one strain would be present in larger numbers. To compensate for this, we here mixed the different overnight cultures such that similar
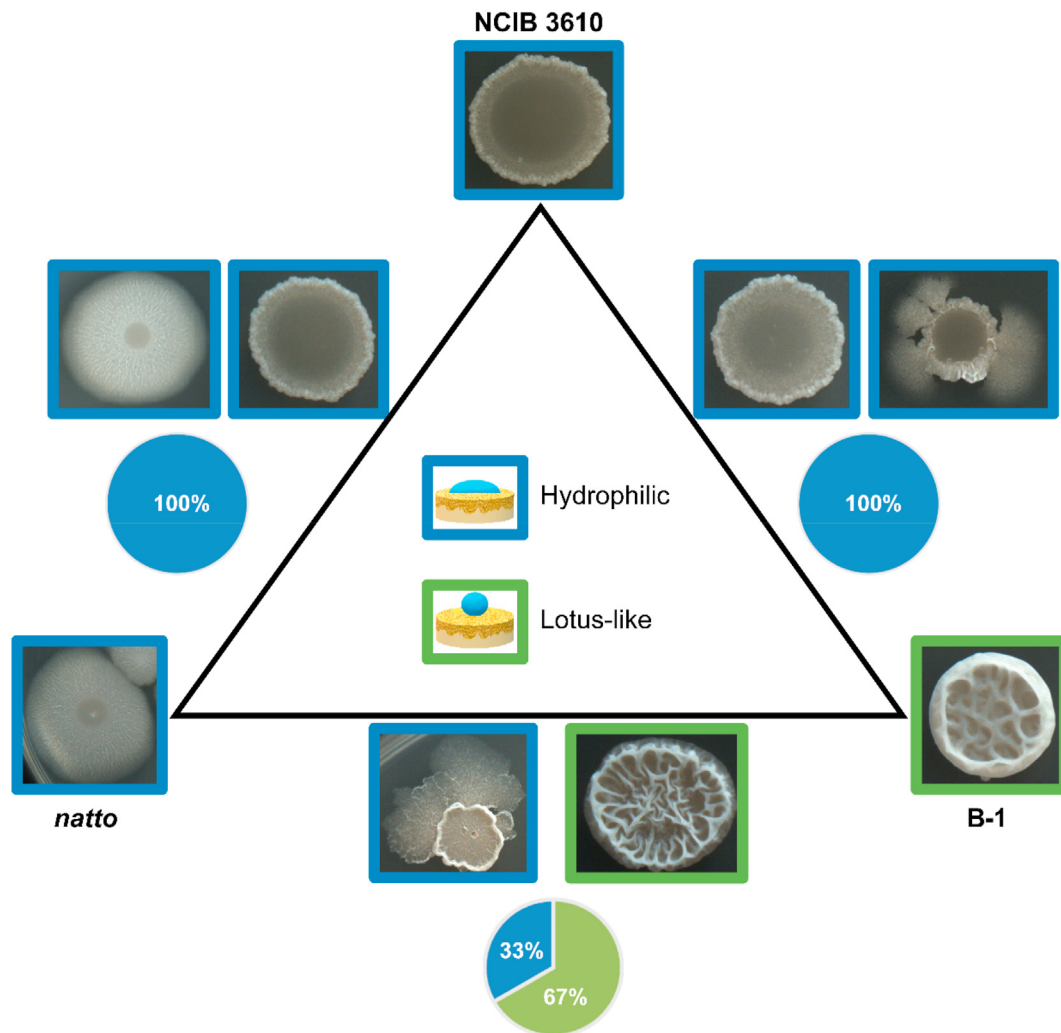
Fig. 1. Overview of single-species and binary mixtures of co-cultured *B. subtilis* NCIB 3610, *natto* and B-1 biofilm colonies grown on LB agar. In each corner of the triangle, a typical example of a single strain colony is shown; in between, example images of mixture colonies are shown. The color of the image frames denotes the wetting behavior of the respective biofilm colonies; hydrophilic biofilms are indicated in blue and lotus-like superhydrophobic biofilms in green, respectively. The pie charts below the images describe the frequency at which the different wetting behaviors occur. Wetting tests on co-cultivated biofilm samples are conducted on 15 colonies grown from 3 different batches. (For interpretation of the references to color in this figure legend, the reader is referred to the Web version of this article.)

numbers of CFUs from each strain were added to the inoculation mix. With this approach, we generate all possible binary mixtures of *B. subtilis* NCIB 3610, *natt*o and B-1 bacteria.

For the colonies produced by those mixtures, a panel consisting of nine people (none of whom took part in the experiments shown here) is asked to classify the morphology of the colonies (Table S1) by comparing their macroscopic appearance to that of colonies generated by one of the 'parent' strains. In addition to the panel survey, we also employ computational approaches to select the most similar 'parent' strain for each co-cultured daughter colony (see Methods section and supplementary information). Among these three image categorization approaches (i.e., algorithms applying 'structural similarity', 'template matching' and 'feature detection' methods), we consider the 'feature detection' approach to be the most reliable one. This assessment is based on our observation that this particular algorithm returns the lowest amount of clearly wrong assignments, i.e., it only rarely selects 'dominant' strains that are not even present in the co-cultured biofilm colonies. Interestingly, such a clearly wrong assignment never occurred in the panel decisions. Based on this result, we conclude that the panel assessments are more reasonable than the algorithm-based categorization results – yet, the panel decisions are not fully correct either (Fig. 2). Nevertheless, for the remainder of this article, we use the categorizations obtained by the

panel evaluations to sort the 'daughter' colonies for further micromorphological investigations.

As depicted in Table S1, binary mixtures containing *B. subtilis* NCIB 3610 and B-1 bacteria are all rated by the panel to be dominated by the NCIB 3610 strain. In agreement with this panel assessment, all those colonies show hydrophilic surfaces with contact angles typical for pure NCIB 3610 colonies cultivated at those conditions (Fig. 3a).

Of course, all information discussed so far has been obtained on a macroscopic scale. Yet, it has been shown in several previous studies, that the wetting properties of bacterial biofilms are controlled on a microscopic level which cannot be visualized by simple, macroscopic camera images. Yet, microscopic imaging techniques such as laser scanning profilometry (a variant of confocal light microscopy) allow for accessing this microscopic length scale, and they provide topographical information that can be quantified by metrological parameters. Examples of such topographical images of both, single-strain 'parent' colonies and mixed 'daughter' colonies are shown in Fig. S4. A quantification of the microscopic surface topographies of mixed colonies returns roughness values (represented by the *Sdr* parameter) that are very similar to those determined for pure NCIB 3610 colonies (Fig. 3d). Taken together, this shows that, for this particular mixture of strains, the panel evaluation can correctly identify the main contributor responsible for the surface
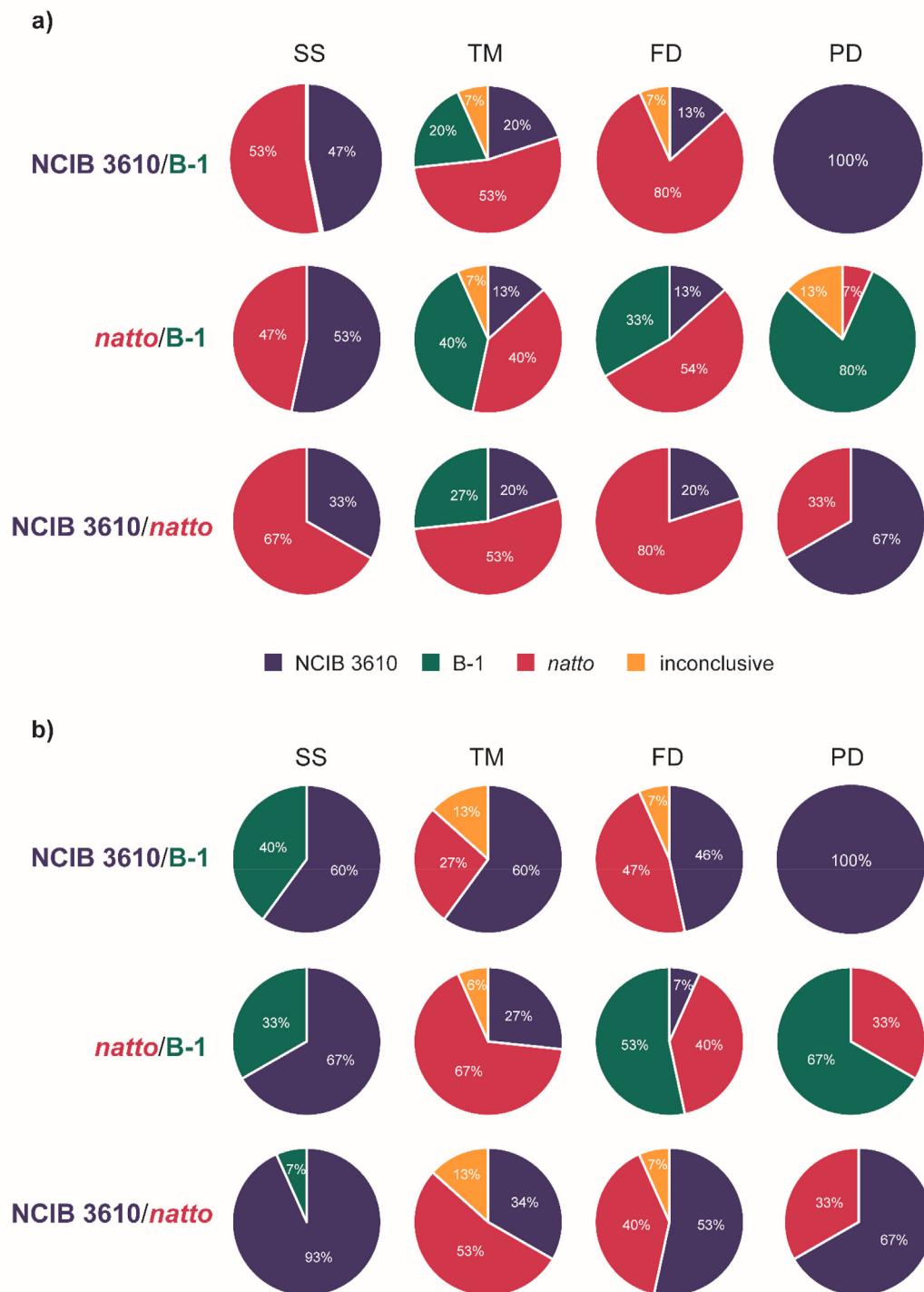
Fig. 2. Biofilm colony classifications based on panel decisions (PD) and computational methods evaluating the macromorphological appearance of the co-cultured colonies. The three algorithms make use of structural similarity (SS), template matching (TM) and feature detection (FD) equations (see SI for details). The pie charts depict pooled results from 15 co-cultured colonies grown on LB (a) and MSgg agar (b).

properties of the mixed colony. For binary mixtures of *natto* and B-1 bacteria, a more complex picture emerges. Here, whereas the majority of colonies seems to be morphologically dominated by B-1, the panel rates some colonies as "*natto*-like" or even "NCIB 3610-like" (Table S1). This result shows that, for colonies generated by this mixture of bacterial strains, a more detailed analysis is required. A wetting analysis of the colonies shows that the majority of colonies have hydrophobic surfaces similar to those present on pure B-1 colonies; however, a subset of samples has hydrophilic surface properties similar to those of pure *natto*

colonies (Figs. 1 and 3b). In agreement with this observation, also an analysis of the microscopic surface topography of the mixed colonies allows for sorting them into two sub-groups: the hydrophilic (*natto*-like) colonies have low *Sdr* values around 100% whereas the hydrophobic (B-1-like) colonies exhibit high *Sdr* values on the order of ~1000%. Interestingly, we find a significant increase in this microscopic surface roughness parameter for the *natto*-like mixture colonies compared to pure *natto* colonies (Fig. 3e). Similarly, the average contact angle of B-1-like colonies is slightly but significantly lower than the corresponding
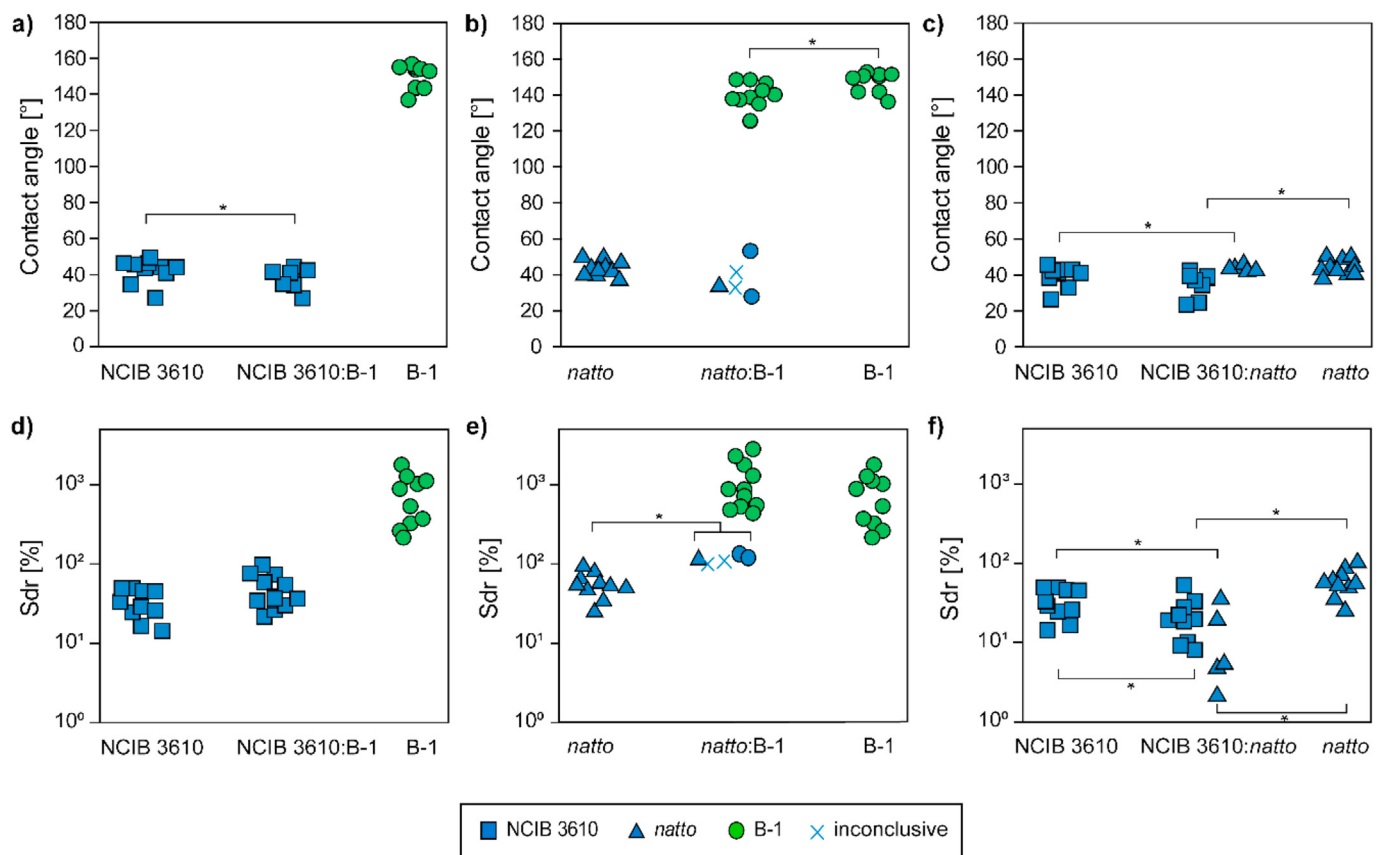
Fig. 3. Quantitative characterization of different biofilm colonies grown on LB agar. Contact angle and surface roughness (*Sdr*) values are obtained on the center biofilm colonies generated from co-cultured NCIB 3610/B-1 (**a,d**), *natto*/B-1 (**b,e**) and NCIB 3610/*natto* (**c,f**) colonies and compared to values obtained from single-strain colonies. Each symbol denotes the average value of three technical replicates obtained from one colony. The data is sorted according to the panel decision regarding the morphological dominance of either NCIB 3610 (□), *natto* (△) or B-1 (○) in the co-cultured colonies. If the panel voting did not lead to a conclusive result, those colonies are indicated by a cross (X). The detailed wetting behavior of the biofilm colonies is indicated by the color of the marker: green color represents lotus-like superhydrophobic behavior and blue color represents hydrophilic behavior. Asterisks denote statistical significances based on a *p*-value of $p = 0.05$. Even though we find significant differences between the contact angles and *Sdr* values of all single-strain 'parent' colonies (when compared pair-wise), this is not marked in the figure for simplicity. (For interpretation of the references to color in this figure legend, the reader is referred to the Web version of this article.)

value we determine for pure B-1 colonies (Fig. 3b). Together, this indicates that, in this particular mixture scenario, there are two possible experimental outcomes: either *natto* or B-1 can dominate in the 'daughter' colonies. Moreover, even though the main contributor to the colony properties can be clearly identified in both cases, the presence of the other bacterial strain influences the colony properties as well – albeit subtly.

The third binary mixture we study is a co-cultivation of *B. subtilis* NCIB 3610 and *natto* bacteria. Here, the panel considers 2/3 of the 'daughter' colonies to be morphologically dominated by NCIB 3610, and the remaining third mostly as *natto*-dominated (Table S1). Since both 'parent' colonies are hydrophilic, so are all the daughter colonies (Fig. 1). Still, the contact angles we determine on the daughter colonies allow for a categorization into 3610-like (CA = $38° \pm 5°$) and *natto*-like (CA = $43° \pm 4°$), with the average CA value of each subpopulation being significantly different from the CA-value typical for the 'other' (= not dominant) parent (Fig. 3c). Interestingly, both of the daughter colony variants exhibit less pronounced surface roughness features (*Sdr*) than their parents (Fig. 3f). This is somewhat unexpected as the contact angles of the two daughter subpopulations agree very well with those determined for the dominating parent colony. Moreover, with a reverse approach, i.e., by conducting a pair-wise comparison of contact angles determined for both, individual NCIB 3610/*natto* mixture colonies and each of the three putative mother strain colonies, good agreement with the panel decisions is obtained (Table S2). In contrast, when the *Sdr* data is used for a similar identification approach, lots of wrong assignments are obtained. This

indicates that, for such a reverse assignment of parent strains, a more detailed analysis of the surface topography is required – most likely including more than only one metrological parameter. A more detailed analysis of the surface features of those daughter colonies suggests the following explanation: as the daughter and parent colonies have very similar peak, core and valley heights but the peak density is lower for the daughter colonies, the same wetting behavior occurs even though the surface roughness parameter *Sdr* is reduced (Table S3).

So far, we have shown that binary mixtures of *B. subtilis* NCIB 3610, *natto* and B-1 strains generate biofilm colonies with surface features (contact angles and surface roughness) that resemble those of one of their parent colonies but are nevertheless significantly different. This suggests that the other, morphologically non-dominant parent strain has a relevant influence on the colony properties. For this influence to manifest, of course, the 'other' parent strain has to be present in the daughter colony, i.e., it must not be outgrown by the second strain it is co-cultured with. Indeed, growth curves obtained for the three *B. subtilis* strains in liquid LB medium (Fig. 4a) already indicate that this is most likely not the case: when grown in parallel at identical conditions, NCIB 3610 bacteria do not possess a growth advantage over the other strains; yet, they clearly dominate the properties of, e.g., colonies where they are mixed with B-1 bacteria. Similarly, the growth curve we obtain for B-1 bacteria indicates slightly slower growth kinetics than what we obtain for *natto* - but mixed colonies created from those two strains tend to be morphologically dominated by B-1.

Hence, as a next step, we aim to verify the coexistence of both parent

a)

b)
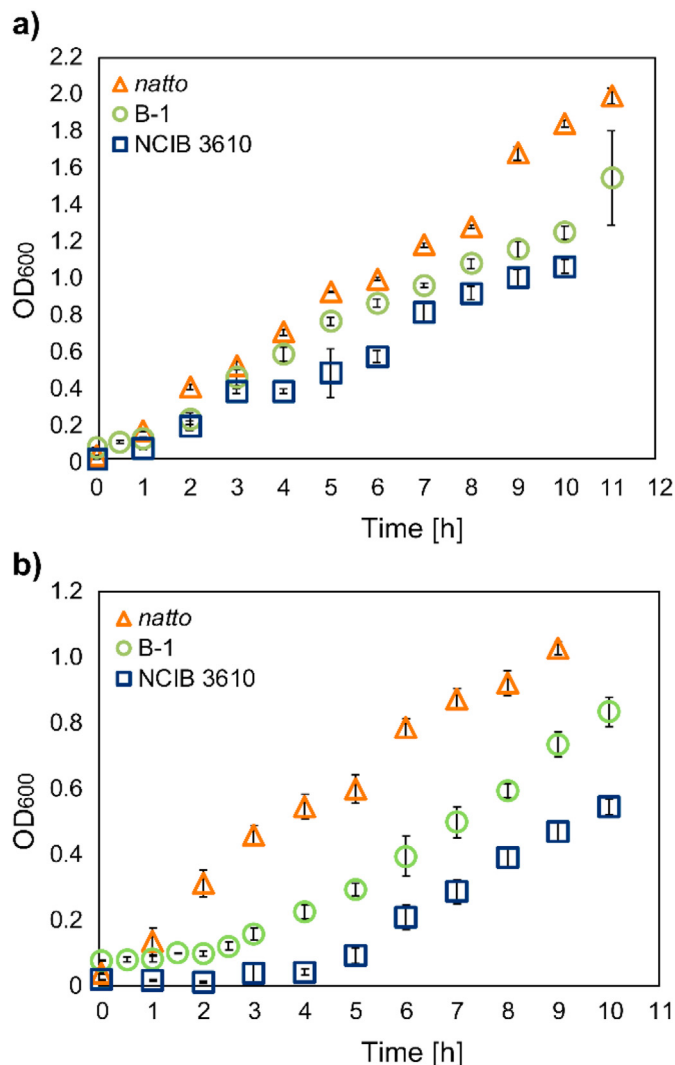
Fig. 4. Microbial growth of planktonic *B. subtilis* NCIB 3610, *natto* and B-1 bacteria at 37 °C. Growth in LB (a) and MSgg (b) media is quantified by determining the optical density (OD$_{600}$). Error bars indicate the standard deviation as obtained from 3 biological replicates.

strains in the daughter colonies by using a fluorescent (GFP expressing) NCIB 3610 strain. Both, in colonies created from NCIB 3610/B-1 and NCIB 3610/*natto* mixtures, the strongly green appearance of the colonies already demonstrates the presence of the NCIB 3610 strain – in full agreement with our expectation (as this strain was the dominant parent in both cases). Moreover, when we quantify the ratio of GFP-labeled (= NCIB 3610) to non-fluorescent (= either *natto* or B-1) bacteria in the center of each colony by a combination of fluorescence and phase-contrast microscopy (see Methods), we can always detect a significant content of the second parent strain: for NCIB 3610/B-1 colonies, this content can vary between 1% and 22%; although this is very low, it seems to be sufficient to influence the surface properties of the daughter colonies. For NCIB 3610/*natto* mixtures, the relative content of the 'other' parent (= *natto*) is much higher and ranges from 24% to 79% (Fig. 5a). This variation is quite high which may seem surprising. However, when the results are sorted into the same two subpopulations we identified above, this large variation in the relative content of the two bacteria agrees very well with our previous assessment: '*natt*o-like' daughter colonies contain predominantly *natto* bacteria, whereas 'NCIB 3610-like' colonies contain mostly NCIB 3610 bacteria.

To investigate whether the two parent strains still co-exist at the periphery of the daughter colonies, we quantify the ratio of GFP-labeled

a)

b)
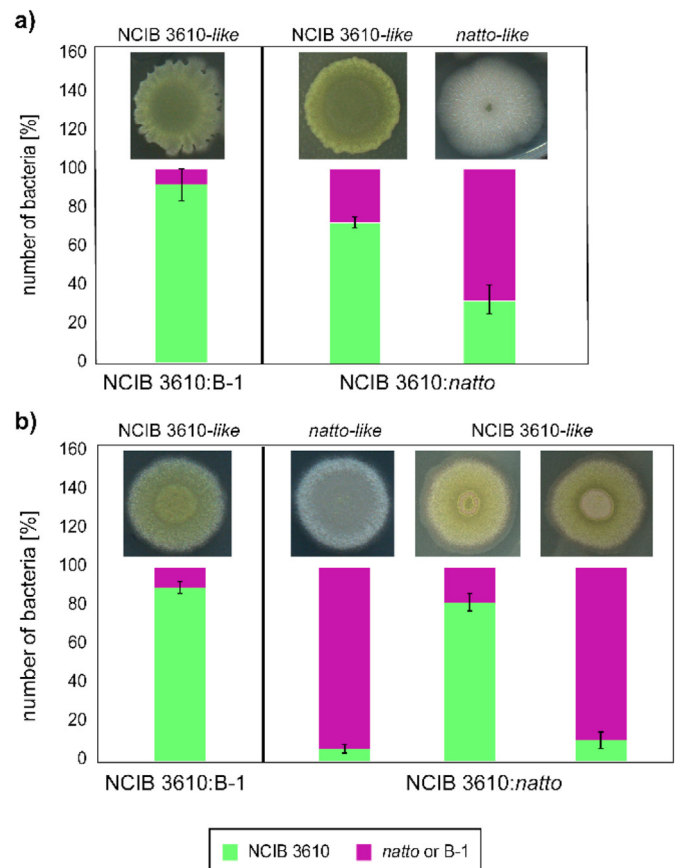
Fig. 5. Strain identification in the center of co-cultured *B. subtilis* biofilm colonies as assessed by fluorescence microscopy. The coexistence ratio of fluorescent NCIB 3610 bacteria and another, non-fluorescent strain (either *natto* or B-1) is shown for different sub-groups (see main text) of co-cultured biofilm colonies grown on LB (a) and MSgg (b) agar. Error bars represent the standard deviation as obtained from at least 5 different colonies.

and other bacteria at the peripheral part of such daughter colonies, where we detect a different macroscopic structure than in the colony center (Fig. S5). By doing so, we find that the morphologically dominating strain is also present at higher numbers in those colony peripheries. Furthermore, similar to what we described above for the central areas of co-cultured biofilm colonies, we find clear indications that, also in those peripheral regions, both strains contribute to the surface roughness features of the daughter colony (Fig. S5).

So far, we showed that the coexistence of both parent strains in the daughter colonies leads to biofilms with hybrid surface properties that are brought about by both parent strains. In the experiments discussed above, a nutrient-rich medium, i.e., LB, was chosen for biofilm growth. However, a different scenario might emerge when the range of available nutrients is limited [53]: the range of nutrients available during biofilm growth not only affects bacterial interactions [31], also the properties of single strain *B. subtilis* biofilms depend on the nutrient conditions: for instance, biofilms can show different surface topographies and wetting behaviors when generated at nutrient-rich and limiting nutrient conditions, respectively [8]. Hence, in a next step, we repeated the co-cultivation experiments using MSgg medium as a nutrient source.

As expected, we observe a different growth behavior for the plank-tonic bacteria in MSgg medium, where the only carbon source is glycerol. As for B-1 bacteria, the planktonic growth of NCIB 3610 bacteria shows a long (~5 h) lag phase at the conditions chosen here (see Methods). The limited nutrient sources available in MSgg medium increase the gaps between the planktonic growth curves of *B. subtilis* NCIB 3610, *natto* and B-1 strains (Fig. 4b); overall, *natto* bacteria seem to have a clear

advantage over the other strains (due to the short lag-phase). Thus, naively, one might assume that *natto* bacteria will always dominate the other two strains in co-cultured biofilm colonies; however, as we show below, this is not necessarily the case.

When the three *B. subtilis* strains are individually grown on MSgg agar, the generated colonies show three different modes of wetting (Fig. 6): B-1 colonies again exhibit lotus-like superhydrophobic surfaces with very high contact angles (CA = $142° \pm 6°$) and *Sdr* values in the range of ~1000% (Fig. 7). Also *natto* colonies have similar (= hydrophilic) surface properties as when grown on LB agar, with both, low *Sdr* and CA values alike. NCIB 3610 colonies, however, now possess strongly hydrophobic surfaces (CA = $138° \pm 4°$) with water-adhesive properties – a combination that is referred to as 'rose-like' superhydrophobicity [3]. Consistent with previous results, this is reflected by intermediate surface roughness values (*Sdr* =(120 ± 7)%), which are significantly different from both, the surface roughness of B-1 and *natto* colonies grown on MSgg agar at the conditions chosen here. We would like to mention, that the capability of NCIB 3610 and B-1 strains to generate superhydrophobic colonies is intimately linked to their ability to express the hydrophobic surface layer protein *BslA* [11] – a property that *natto* bacteria lack. Here, we tested the contribution of this hydrophobin *BslA* to the surface hydrophobicity of co-cultured colonies by employing a NCIB 3610 mutant strain unable to produce *BslA* (*ΔBslA*). Indeed, in full agreement with results described in the literature [12,21,22,54–58], co-cultivation of *ΔBslA* with one of the other strains results in hydrophilic daughter colonies (Fig. S7).

For biofilm colonies grown from binary strain mixtures on MSgg agar, we obtain an outcome that supports our findings obtained on LB agar: daughter colonies that morphologically resemble one of their mother colonies also show wetting properties that agree with this morphological similarity (Fig. 6). However, now, the panel participants are able to identify the dominating 'mother' strain with higher accuracy (Table S1). A more detailed analysis of the colony properties shows that the contact angles we measure for co-cultured colonies are always virtually identical to those we measure on the dominating 'mother' colony (Fig. 7a–c). As determining static contact angles is not sufficient to distinguish between rose-like and lotus-like superhydrophobic surfaces [3,4], the categorization applied to samples showing high contact angles >120° is conducted by tilting the samples with a wetting droplet on their surface (as described above). Yet, based on this contact angle analysis alone, a clear contribution of the non-dominant parent strain is, so far, not evident.

Such a contribution, however, becomes detectable when the microscopic surface roughness of the colonies is analyzed. Similar to when they are grown on LB agar, NCIB 3610-like and *natto*-like daughter colonies grown on MSgg agar exhibit a slightly (but significantly) different surface topography compared to colonies formed by their dominating parent. For NCIB-3610/B-1 mixtures and *natto*/B-1 mixtures, analyzing the *Sdr* values is sufficient to make this statement (Fig. 7d–f); for NCIB 3610/*natto* mixtures, however, the topography of the daughter colonies is more complicated and requires the analysis of more complex metrological surface parameters to identify the contribution of the non-dominating parent (Table S4). Only for B-1-like daughter colonies, we cannot detect such a clear contribution of the non-dominating parent (Fig. 7d and e); we speculate that this is due to wide distribution of *Sdr* values (and other roughness parameters) we obtain for those lotus-like colonies. As in previous studies, where the surface roughness of B-1 biofilm colonies was quantified, the *Sdr* values obtained from those particular biofilms cover a very broad range [10,11]. In addition to the occurrence of roughness features on several length scales, another main reason for the wide distribution of those values is the random selection of areas on the
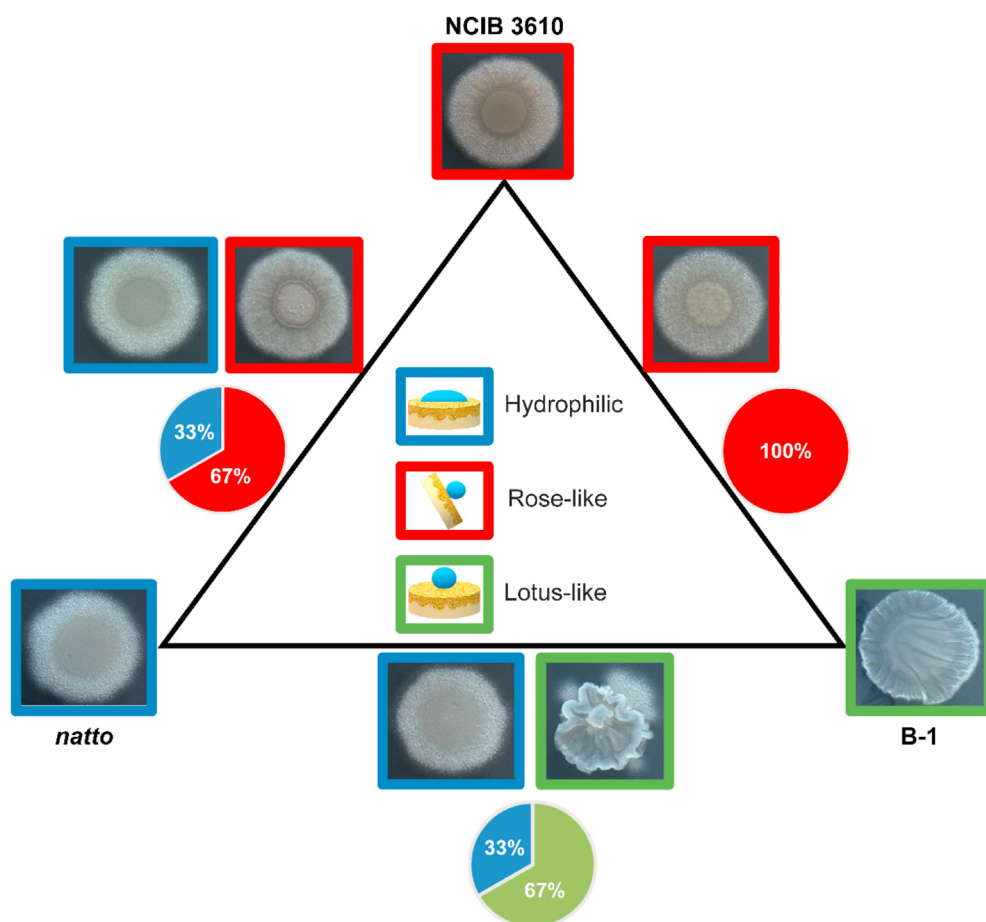
Fig. 6. Overview of single-species and binary mixtures of co-cultured *B. subtilis* NCIB 3610, *natto* and B-1 biofilm colonies grown on MSgg agar. In each corner of the triangle, a typical example of a single strain colony is shown; in between, example images of mixture colonies are shown. The color of the image frames denotes the wetting behavior of the respective biofilm colonies; hydrophilic biofilms are indicated in blue, rose-like superhydrophobic biofilms in red, and lotus-like superhydrophobic biofilms in green. The pie charts below the images describe the frequency at which the different wetting behaviors occur. Wetting tests on co-cultivated biofilm samples are conducted on at least 15 colonies grown from 3 different batches. (For interpretation of the references to color in this figure legend, the reader is referred to the Web version of this article.)
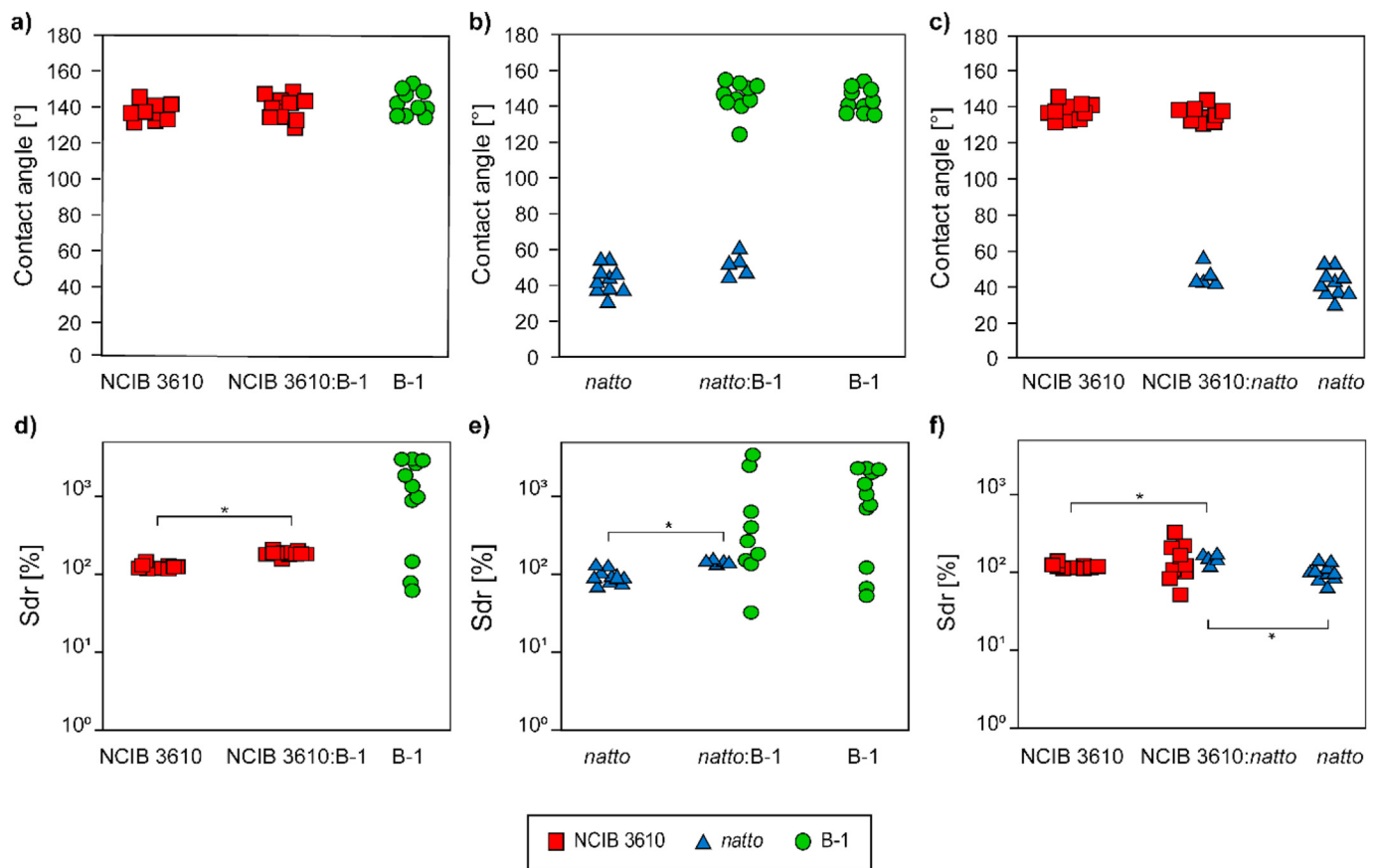
Fig. 7. Quantitative characterization of different biofilm colonies grown on MSgg agar. Contact angle and surface roughness (*Sdr*) values are obtained on the center biofilm colonies generated from co-cultured NCIB 3610/B-1 (**a,d**), *natto*/B-1 (**b,e**) and NCIB 3610/*natto* (**c,f**) colonies and compared to values obtained from single-strain colonies. Each symbol denotes the average value of three technical replicates obtained from one colony. The data is sorted according to the panel decision regarding the morphological dominance of either NCIB 3610 (□), *natto* (△) or B-1 (○) in the co-cultured colonies. The detailed wetting behavior of the biofilm colonies is indicated by the color of the marker: green color represents lotus-like superhydrophobic behavior, red color indicates rose-like superhydrophobic behavior, and blue color represents hydrophilic behavior. Asterisks denote statistical significances based on a *p*-value of $p = 0.05$. Even though we find significant differences between the contact angles and *Sdr* values of all single-strain 'parent' colonies (when compared pair-wise), this is not marked in the figure for simplicity. (For interpretation of the references to color in this figure legend, the reader is referred to the Web version of this article.)

biofilm colony for microscopic surface roughness analysis – some of which took place on local valleys of the macroscopic waves, some of which on the top of those macro-structures.

As for the results we discuss above for colonies grown on LB agar, also for co-cultured colonies grown on MSgg agar we can confirm that both parent strains coexist (Fig. 5b). Interestingly, we find two realizations of NCIB 3610-like daughters of NCIB 3610/*natto* mixtures: in one case, the mixture contains mainly (i.e., ~82%) NCIB 3610 bacteria. However, in a second subgroup, we detected mostly (i.e., ~89%) *natto* bacteria (Fig. 5b). Most likely, the panel rated both of those colony variants generated by this particular mixture as 'NCIB 3610-like' since the periphery structure of those colonies shows a macroscopic morphology typical for NCIB 3610 colonies (Table S1). Moreover, the wetting behavior of both of those subgroups is identical to that of NCIB 3610 colonies, i.e. rose-like with a wide distribution of *Sdr* values (Fig. 7c, f). Thus, in this particular case, although it 'looks like a duck and swims like a duck and quacks like a duck – it's a goose-duck' [59].

Conclusions

For the conditions we study here, co-cultured biofilm colonies are always – in terms of numbers – dominated by one parent strain, and this dominating strain is mostly responsible for the macro- and microscopic morphology of the daughter colony. However, these daughter colonies are also significantly (and measurably) influenced by the other parent strain. These findings show that the presence of a second bacterial strain

– even at relatively small amounts – may cause slight but significant changes in the properties of a biofilm. Whether or not the two co-cultured bacteria are well-mixed on a microscopic scale, or if they grow in local niches (e.g., on top of each other), is – at this point of research, not clear yet. Nevertheless, our insights may provide useful stimuli for biotechnological applications where biofilms are engineered to possess dedicated properties: As we show it here for using *B. subtilis* bacteria, a desired property present in a single-strain biofilm may be transferred to a multi-species biofilm by co-cultivation of different bacteria – provided that the different bacteria can exist together without extinguishing each other.

CRediT authorship contribution statement

Elif N. Hayta: Conceptualization, Methodology, Investigation, Formal analysis, Writing - original draft, Visualization, Funding acquisition. **Carolin A. Rickert:** Software, Formal analysis, Writing - original draft. **Oliver Lieleg:** Conceptualization, Methodology, Resources, Writing - review & editing, Visualization, Supervision, Funding acquisition.

Declaration of competing interest

The authors declare that they have no known competing financial interests or personal relationships that could have appeared to influence the work reported in this paper.

Appendix A. Supplementary data

Supplementary data to this article can be found online at https://doi.org/10.1016/j.biofilm.2021.100044.

References

[1] Edmunds M. On the association between Myrmarachne spp. (Salticidae) and ants. Bull Br Arachnol Soc 1978;4:149–60.

[2] Shamble PS, Hoy RR, Cohen I, Beatus T. Walking like an ant: a quantitative and experimental approach to understanding locomotor mimicry in the jumping spider Myrmarachne formicaria. Proc R Soc B Biol Sci 2017;284:20170308. https://doi.org/10.1098/rspb.2017.0308.

[3] Bhushan B, Nosonovsky M. The rose petal effect and the modes of superhydrophobicity. Philos Trans R Soc A Math Phys Eng Sci 2010;368:4713–28. https://doi.org/10.1098/rsta.2010.0203.

[4] Wang S, Jiang L. Definition of superhydrophobic states. Adv Mater 2007;19:3423–4. https://doi.org/10.1002/adma.200700934.

[5] Shim MH, Kim J, Park CH. The effects of surface energy and roughness on the hydrophobicity of woven fabrics. Textil Res J 2014;84:1268–78. https://doi.org/10.1177/0040517513495945.

[6] Erbil HY, Demirel AL, Avci Y, Mert O. Transformation of a simple plastic into a superhydrophobic surface. Science 2003;299:1377–80. https://doi.org/10.1126/science.1078365. 80.

[7] Nosonovsky M, Bhushan B. Hierarchical roughness optimization for biomimetic superhydrophobic surfaces. Ultramicroscopy 2007;107:969–79. https://doi.org/10.1016/j.ultramic.2007.04.011.

[8] Werb M, Falcón García C, Bach NC, Grumbein S, Sieber SA, Opitz M, Lieleg O. Surface topology affects wetting behavior of Bacillus subtilis biofilms. Npj Biofilms Microbiomes 2017;3:11. https://doi.org/10.1038/s41522-017-0018-1.

[9] Hayta EN, Lieleg O. Biopolymer-enriched: B. subtilis NCIB 3610 biofilms exhibit increased erosion resistance. Biomater Sci 2019;7:4675–86. https://doi.org/10.1039/c9bm00927b.

[10] Falcón García C, Stangl F, Götz A, Zhao W, Sieber SA, Opitz M, Lieleg O. Topographical alterations render bacterial biofilms susceptible to chemical and mechanical stress. Biomater Sci 2019;7:220–32. https://doi.org/10.1039/c8bm00987b.

[11] Kesel S, Grumbein S, Tallawi M, Marel A, Lieleg O, Opitz M. Direct comparison of physical properties of Bacillus subtilis NCIB 3610 and B-1 biofilms. Appl Environ Microbiol 2016;82:2424–32. https://doi.org/10.1128/AEM.03957-15.

[12] Kesel S, Von Bronk B, Falcón García C, Götz A, Lieleg O, Opitz M. Matrix composition determines the dimensions of: Bacillus subtilis NCIB 3610 biofilm colonies grown on LB agar. RSC Adv 2017;7:31886–98. https://doi.org/10.1039/c7ra05559e.

[13] Raab N, Bachelet I. Resolving biofilm topography by native scanning electron microscopy. J Biol Methods 2017;4:70. https://doi.org/10.14440/jbm.2017.173.

[14] Huang Y, Chakraborty S, Liang H. Methods to probe the formation of biofilms: applications in foods and related surfaces. Anal Methods 2020;12:416–32. https://doi.org/10.1039/c9ay02214g.

[15] Schiebel J, Noack J, Rödiger S, Kammel A, Menzel F, Schwibbert K, Weise M, Weiss R, Böhm A, Nitschke J, Elimport A, Roggenbuck D, Schierack P. Analysis of three-dimensional biofilms on different material surfaces. Biomater Sci 2020;8:3500–10. https://doi.org/10.1039/d0bm00455c.

[16] Klotz M, Kretschmer M, Goetz A, Ezendam S, Lieleg O, Opitz M. Importance of the biofilm matrix for the erosion stability of Bacillus subtilis NCIB 3610 biofilms. RSC Adv 2019;9:11521–9. https://doi.org/10.1039/C9RA01955C.

[17] T RJ, Marc JH, Demeter A, Lemire Joseph A. Biofilm survival strategies in polluted environments. In: Lear G, editor. Biofilms Bioremediation Curr. Res. Emerg. Technol., Caister Academic Press, Norfolk, UK; 2016. p. 43–57.

[18] Branda SS, Chu F, Kearns DB, Losick R, Kolter R. A major protein component of the Bacillus subtilis biofilm matrix. Mol Microbiol 2006;59:1229–38. https://doi.org/10.1111/j.1365-2958.2005.05020.x.

[19] Kearns DB, Chu F, Branda SS, Kolter R, Losick R. A master regulator for biofilm formation by Bacillus subtilis. Mol Microbiol 2005;55:739–49. https://doi.org/10.1111/j.1365-2958.2004.04440.x.

[20] Romero D, Aguilar C, Losick R, Kolter R. Amyloid fibers provide structural integrity to Bacillus subtilis biofilms. Proc Natl Acad Sci USA 2010;107:2230–4. https://doi.org/10.1073/pnas.0910560107.

[21] Kobayashi K, Iwano M. BslA(YuaB) forms a hydrophobic layer on the surface of Bacillus subtilis biofilms. Mol Microbiol 2012;85:51–66. https://doi.org/10.1111/j.1365-2958.2012.08094.x.

[22] Hobley L, Ostrowski A, Rao FV, Bromley KM, Porter M, Prescott AR, MacPhee CE, Van Aalten DMF, Stanley-Wall NR. BslA is a self-assembling bacterial hydrophobin that coats the Bacillus subtilis biofilm. Proc Natl Acad Sci USA 2013;110:13600–5. https://doi.org/10.1073/pnas.1306390110.

[23] Morikawa M, Kagihiro S, Haruki M, Takano K, Branda S, Kolter R, Kanaya S. Biofilm formation by a Bacillus subtilis strain that produces γ-polyglutamate. Microbiology 2006;152:2801–7. https://doi.org/10.1099/mic.0.29060-0.

[24] Kimura K, Phan Tran LS, Do TH, Itoh Y. Expression of the pgsB Encoding the poly-gamma-DL-glutamate synthetase of bacillus subtilis (natto). Biosci Biotechnol Biochem 2009;73:1149–55. https://doi.org/10.1271/bbb.80913.

[25] Bowen WH, Burne RA, Wu H, Koo H. Oral biofilms: pathogens, matrix, and polymicrobial interactions in microenvironments. Trends Microbiol 2018;26:229–42. https://doi.org/10.1016/j.tim.2017.09.008.

[26] Lamont RJ, Hajishengallis G. Polymicrobial synergy and dysbiosis in inflammatory disease. Trends Mol Med 2015;21:172–83. https://doi.org/10.1016/j.molmed.2014.11.004.

[27] Marsh PD, Head DA, Devine DA. Dental plaque as a biofilm and a microbial community - implications for treatment. J Oral Biosci 2015;57:185–91. https://doi.org/10.1016/j.job.2015.08.002.

[28] Karygianni L, Ren Z, Koo H, Thurnheer T. Biofilm matrixome: extracellular components in structured microbial communities. Trends Microbiol 2020;28:668–81. https://doi.org/10.1016/j.tim.2020.03.016.

[29] Lazarova V, Manem J. Biofilm characterization and activity analysis in water and wastewater treatment. Water Res 1995;29:2227–45. https://doi.org/10.1016/0043-1354(95)00054-O.

[30] Hassard F, Biddle J, Cartmell E, Jefferson B, Tyrrel S, Stephenson T. Rotating biological contactors for wastewater treatment - a review. Process Saf Environ Protect 2015;94:285–306. https://doi.org/10.1016/j.psep.2014.07.003.

[31] Ghoul M, Mitri S. The ecology and evolution of microbial competition. Trends Microbiol 2016;24:833–45. https://doi.org/10.1016/j.tim.2016.06.011.

[32] Røder HL, Sørensen SJ, Burmølle M. Studying bacterial multispecies biofilms: where to start? Trends Microbiol 2016;24:503–13. https://doi.org/10.1016/j.tim.2016.02.019.

[33] Burmølle M, Ren D, Bjarnsholt T, Sørensen SJ. Interactions in multispecies biofilms: do they actually matter? Trends Microbiol 2014;22:84–91. https://doi.org/10.1016/j.tim.2013.12.004.

[34] Zuo R, Wood TK. Inhibiting mild steel corrosion from sulfate-reducing and iron-oxidizing bacteria using gramicidin-S-producing biofilms. Appl Microbiol Biotechnol 2004;65:747–53. https://doi.org/10.1007/s00253-004-1651-1.

[35] Jayaraman A, Hallock PJ, Carson RM, Lee CC, Mansfeld FB, Wood TK. Inhibiting sulfate-reducing bacteria in biofilms on steel with antimicrobial peptides generated in situ. Appl Microbiol Biotechnol 1999;52:267–75. https://doi.org/10.1007/s002530051520.

[36] Singh R, Sahore S, Kaur P, Rani A, Ray P. Penetration barrier contributes to bacterial biofilm-associated resistance against only select antibiotics, and exhibits genus-, strain- and antibiotic-specific differences. Pathog Dis 2016;74:2–7. https://doi.org/10.1093/femspd/ftw056.

[37] Kinkel LL, Schlatter DC, Xiao K, Baines AD. Sympatric inhibition and niche differentiation suggest alternative coevolutionary trajectories among Streptomycetes. ISME J 2014;8:249–56. https://doi.org/10.1038/ismej.2013.175.

[38] Coyte KZ, Tabuteau H, Gaffney EA, Fostera KR, Durham WM. Microbial competition in porous environments can select against rapid biofilm growth. Proc Natl Acad Sci USA 2017;114:E161–70. https://doi.org/10.1073/pnas.1525228113.

[39] Liu J, Prindle A, Humphries J, Gabalda-Sagarra M, Asally M, Lee DYD, Ly S, Garcia-Ojalvo J, Süel GM. Metabolic co-dependence gives rise to collective oscillations within biofilms. Nature 2015;523:550–4. https://doi.org/10.1038/nature14660.

[40] Liu W, Røder HL, Madsen JS, Bjarnsholt T, Sørensen SJ, Burmølle M. Interspecific bacterial interactions are reflected in multispecies biofilm spatial organization. Front Microbiol 2016;7:1–8. https://doi.org/10.3389/fmicb.2016.01366.

[41] Paul R, Ghosh T, Tang T, Kumar A. Rivalry in: Bacillus subtilis colonies: enemy or family? Soft Matter 2019;15:5400–11. https://doi.org/10.1039/c9sm00794f.

[42] Matoz-Fernandez D, Arnaouteli S, Porter M, MacPhee CE, Stanley-Wall NR, Davidson FA. Comment on "rivalry in: Bacillus subtilis colonies: enemy or family? Soft Matter 2020;16:3344–6. https://doi.org/10.1039/c9sm02141h.

[43] Wang Z, Bovik AC, Sheikh HR, Simoncelli EP. Image quality assessment: from error visibility to structural similarity. IEEE Trans Image Process 2004;13:600–12. https://doi.org/10.1109/TIP.2003.819861.

[44] Rublee E, Rabaud V, Konolige K, Bradski G. ORB: an efficient alternative to SIFT or SURF. In: Int. Conf. Comput. Vis. IEEE, Barcelona; 2011. p. 2564–71. https://doi.org/10.1109/ICCV.2011.6126544.

[45] Viswanathan DG. Features from accelerated segment test (FAST). In: Proc. 10th work. Image anal. Multimed. Interact. Serv.; 2009. London, UK.

[46] Calonder M, Lepetit V, Strecha C, Fua P. BRIEF: binary robust independent elementary features. Lect Notes Comput Sci (Including Subser Lect Notes Artif Intell Lect Notes Bioinformatics). 6314 LNCS 2010:778–92. https://doi.org/10.1007/978-3-642-15561-1_56.

[47] Harris CR, Millman KJ, van der Walt SJ, Gommers R, Virtanen P, Cournapeau D, Wieser E, Taylor J, Berg S, Smith NJ, Kern R, Picus M, Hoyer S, van Kerkwijk MH, Brett M, Haldane A, del Río JF, Wiebe M, Peterson P, Gérard-Marchant P, Sheppard K, Reddy T, Weckesser W, Abbasi H, Gohlke C, Oliphant TE. Array programming with NumPy. Nature 2020;585:357–62. https://doi.org/10.1038/s41586-020-2649-2.

[48] Bradski G. The OpenCV library. Dr. Dobb's J Softw Tools 2000;25:120–5.

[49] Clark A. Pillow (PIL fork) documentation release 3.1.2. 2020.

[50] van der Walt SJ, Schönberger JL, Nunez-Iglesias J, Boulogne F, Warner JD, Yager N, Gouillart E, Yu T. Scikit-image: image processing in python. PeerJ 2014:1–18. https://doi.org/10.7717/peerj.453. 2014.

[51] Holm S. Board of the foundation of the scandinavian journal of statistics A simple sequentially rejective multiple test procedure author (s): sture holm published by : wiley on behalf of board of the foundation of the scandinavian journal of statistics stable U. Scand J Stat 1978;6:65–70.

[52] Schuler ML, Kargi F. Bioprocess engineering: basic concepts. second ed. Upper Saddle River, NJ: Prentice Hall; 2002.

[53] Gallegos-Monterrosa R, Mhatre E, Kovács ÁT. Specific Bacillus subtilis 168 variants form biofilms on nutrient-rich medium. Microbiol (United Kingdom) 2016;162: 1922–32. https://doi.org/10.1099/mic.0.000371.

[54] Arnaouteli S, MacPhee CE, Stanley-Wall NR. Just in case it rains: building a hydrophobic biofilm the Bacillus subtilis way. Curr Opin Microbiol 2016;34:7–12. https://doi.org/10.1016/j.mib.2016.07.012.

[55] Bromley KM, Morris RJ, Hobley L, Brandani G, Gillespie RMC, McCluskey M, Zachariae U, Marenduzzo D, Stanley-Wall NR, MacPhee CE. Interfacial self-assembly of a bacterial hydrophobin. Proc Natl Acad Sci USA 2015;112:5419–24. https://doi.org/10.1073/pnas.1419016112.

[56] Morris RJ, Schor M, Gillespie RMC, Ferreira AS, Baldauf L, Earl C, Ostrowski A, Hobley L, Bromley KM, Sukhodub T, Arnaouteli S, Stanley-Wall NR, MacPhee CE. Natural variations in the biofilm-associated protein BslA from the genus Bacillus. Sci Rep 2017;7:1–13. https://doi.org/10.1038/s41598-017-06786-9.

[57] Liu W, Li S, Wang Z, Yan ECY, Leblanc RM. Characterization of surface-active biofilm protein BslA in self-assembling Langmuir monolayer at the air-water interface. Langmuir 2017;33:7548–55. https://doi.org/10.1021/acs.langmuir.7b01739.

[58] Kovács ÁT, van Gestel J, Kuipers OP. The protective layer of biofilm: a repellent function for a new class of amphiphilic proteins. Mol Microbiol 2012;85:8–11. https://doi.org/10.1111/j.1365-2958.2012.08101.x.

[59] Riley JW. Poems & Prose Sketches: "When I see a bird that walks like a duck and swims like a duck and quacks like a duck, I call that bird a duck.," Portable Poetry. 2017.